

# ***In Situ* Gravimetric Studies of the Regenerative Mechanism for Water-Gas Shift over Magnetite: Equilibrium and Kinetic Measurements in CO<sub>2</sub>/CO and H<sub>2</sub>O/H<sub>2</sub> Gas Mixtures**

*In situ* gravimetric measurements were used to study oxygen removal from (or incorporation into) chromia-promoted magnetite in CO<sub>2</sub>/CO and H<sub>2</sub>O/H<sub>2</sub> gas mixtures at 637 K. The equilibrium and kinetic data could be described by two reversible, oxidation-reduction reactions: surface-oxygen removal by CO and surface oxygen replenishment by H<sub>2</sub>O, with the corresponding reverse reaction involving CO<sub>2</sub> and H<sub>2</sub>. These reactions form a regenerative mechanism that is able to predict qualitatively both the measured rate and rate expression for water-gas shift. It is concluded that this regenerative mechanism is a primary pathway for water-gas shift over magnetite.

J. E. KUBSH and

J. A. DUMESIC

Department of Chemical Engineering  
University of Wisconsin  
Madison, WI 53706

## **SCOPE**

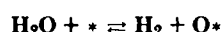
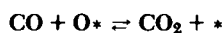
Chromia-promoted magnetite (i.e., Cr<sub>2</sub>O<sub>3</sub>/Fe<sub>3</sub>O<sub>4</sub>) is the preferred catalyst for water-gas shift ( $\text{CO} + \text{H}_2\text{O} \rightleftharpoons \text{CO}_2 + \text{H}_2$ ) at temperatures higher than ca. 620 K. A reaction mechanism that has been effective in describing observed water-gas shift kinetics is the regenerative mechanism, first proposed by Kul'kova and Temkin (1949). Accordingly, the surface of magnetite undergoes successive oxidation and reduction cycles by H<sub>2</sub>O and CO, respectively, with the accompanying formation of H<sub>2</sub> and CO<sub>2</sub>. Boreskov et al. (1970) showed that the rate of water-gas shift is, in fact, approximately equal to the rates at which H<sub>2</sub>O oxidizes and CO reduces the magnetite surface.

In the present study, the validity of the regenerative mechanism for water-gas shift over magnetite is investigated by de-

termining gravimetrically the kinetics and equilibrium extent of surface oxygen removal from (or incorporation into) the catalyst in various CO<sub>2</sub>/CO and H<sub>2</sub>O/H<sub>2</sub> gas mixtures. It is thereby possible to assess the contribution of the regenerative mechanism to the overall rate of water-gas shift, and to determine what fraction of the magnetite surface participates in water-gas shift via this mechanism. Furthermore, by carrying out equilibrium studies in these gas mixtures at different total pressures, the presence of adsorbed species other than surface oxygen (e.g., adsorbed CO and CO<sub>2</sub>) can be probed, and the importance of these species in the regenerative mechanism can be ascertained.

## **CONCLUSIONS AND SIGNIFICANCE**

For chromia-promoted magnetite, the equilibrium extent of surface coverage by oxygen at 637 K was found to depend on the ratios  $P_{\text{CO}_2}/P_{\text{CO}}$  and  $P_{\text{H}_2\text{O}}/P_{\text{H}_2}$ ; and, a given CO<sub>2</sub>/CO gas mixture gave the same surface oxygen coverage as a H<sub>2</sub>O/H<sub>2</sub> mixture, provided that  $P_{\text{CO}_2}/P_{\text{CO}}$  was equal to the product of  $P_{\text{H}_2\text{O}}/P_{\text{H}_2}$  and the equilibrium constant for water-gas shift ( $\text{CO} + \text{H}_2\text{O} \rightleftharpoons \text{CO}_2 + \text{H}_2$ ). These data can be described by the following two reactions:



where O\* and \* are oxygen-containing and vacant surface sites, respectively. Furthermore, these two reactions are able to explain the kinetics of oxygen removal from (or incorporation into)

the surface in these gas mixtures at this temperature. For increasing extents of oxygen removal, the rate of surface oxygen removal by CO and H<sub>2</sub> decreased linearly while the rate of surface oxygen incorporation from CO<sub>2</sub> and H<sub>2</sub>O increased linearly. The maximum amount of surface oxygen that can be removed via these two reactions, however, is only about 9% of the BET monolayer.

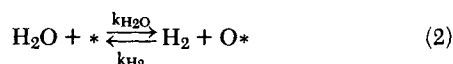
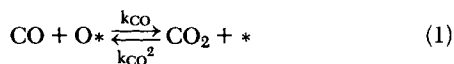
The combination of the above two oxidation-reduction reactions forms a regenerative mechanism that predicts qualitatively both the measured absolute rate and rate expression for water-gas shift over magnetite. Quantitative differences between the predicted and measured rates may be ascribed to effects of surface non-uniformities and/or the presence of adsorbed species other than oxygen. Concerning the latter, an adsorption mechanism for water-gas shift, not involving oxidation-reduction of the surface, may also exist over magnetite. Yet even if both an adsorption and a regenerative mechanism exist, it can be concluded that the regenerative mechanism is an important pathway for water-gas shift over magnetite.

J. A. Dumesic is a Camille and Henry Dreyfus teacher-scholar, to whom correspondence should be addressed.  
0001-1541/82/6108-0793\$2.00. © The American Institute of Chemical Engineers, 1982.

## INTRODUCTION

Although the kinetics of water-gas shift over magnetite-based catalysts ( $\text{Fe}_3\text{O}_4$ ) have been studied extensively (reviews by Bohlbro, 1969; Happel, 1972), the sequence of elementary steps by which the reaction proceeds over such catalysts has not yet been elucidated unambiguously. This is despite the fact that magnetite (structurally promoted by chromia) is an industrial catalyst for high temperature (ca. 650 K) water-gas shift. In short, two types of reaction pathways have been proposed in the literature: adsorption and regenerative mechanisms. In the former pathway, reactants adsorb on the surface where they react to form surface intermediates, followed by decomposition to products and desorption from the surface (Oki et al., 1972). Support for this adsorption mechanism has been provided by tracer studies and apparent stoichiometric number analyses (Kaneko and Oki, 1965; Oki et al., 1972; Oki and Mezaki, 1973) and the corresponding Hougen-Watson models have been effective in fitting reaction kinetics data (Podolski and Kim, 1974). In the regenerative mechanism, the surface of magnetite undergoes successive oxidation and reduction cycles by  $\text{H}_2\text{O}$  and  $\text{CO}$ , respectively, to form the corresponding  $\text{H}_2$  and  $\text{CO}_2$  products of water-gas shift (Kul'kova and Temkin, 1949; Shchibrya et al., 1965). The kinetics of water-gas shift can also be fit very well by this regenerative mechanism (Glavachek et al., 1968). Additional support for this mechanism comes from the work of Boreskov et al. (1970) who showed that the rate of water-gas shift corresponds to the rate at which  $\text{H}_2\text{O}$  oxidizes and  $\text{CO}$  reduces the surface of magnetite. This comparison of rates, however, was not carried out over a range of reactant and product partial pressures.

Because the kinetics of water-gas shift over magnetite can equally well be described by adsorption and regenerative pathways, additional information must be obtained to distinguish these processes. One approach is to determine the kinetics of oxygen removal from, or incorporation into, the surface of magnetite. According to the regenerative mechanism in its simplest form oxidation and reduction of the catalyst occur via the following two steps:



where  $*$  and  $\text{O}^*$  represent vacant and oxygen-containing surface sites, respectively. In the present paper, gravimetric methods and kinetic relaxation techniques are employed at 637 K to determine the individual exchange rates of reactions (Eqs. 1 and 2) over chromia-promoted magnetite in various  $\text{CO}_2/\text{CO}$  and  $\text{H}_2\text{O}/\text{H}_2$  gas mixtures. From such measurements it is possible to predict the rate and rate expression for water-gas shift, which can then be compared to the known kinetics of water-gas shift over magnetite. In addition, it is also possible to determine the surface coverage by  $\text{O}^*$  in the various  $\text{CO}_2/\text{CO}$  and  $\text{H}_2\text{O}/\text{H}_2$  gas mixtures, and to thereby test the implicit assumption in the regenerative mechanism that  $\text{O}^*$  formed in reaction (1) is equivalent to that formed in reaction 2. Finally, the adsorption of species other than  $\text{O}^*$  (e.g., adsorbed  $\text{CO}$  and  $\text{CO}_2$ ) can be studied by combined gravimetric and volumetric methods (as discussed elsewhere (Kubsh et al., 1981), and one can ascertain whether these species influence the rates of reactions (Eqs. 1 and 2). In short, by studying individually the two steps of the regenerative mechanism, it is possible to assess the validity of this mechanism and to determine to what extent it serves as a pathway for water-gas shift over magnetite.

## EXPERIMENTAL

### Strategy for Data Collection

The use of relaxation kinetic measurements as a probe of oxygen or iron oxide surfaces in  $\text{CO}_2/\text{CO}$  and  $\text{H}_2\text{O}/\text{H}_2$  atmospheres has focused mainly

on high temperature studies ( $> 1,000$  K) of wustite ( $\text{FeO}$ ). These oxidation-reduction studies have employed conductive (Stotz, 1966), gravimetric (Riecke and Bohenkamp, 1969) and Auger electron spectroscopy (Grabke and Viehhaus, 1980) measurements. In the particular case of water-gas shift, Stotz (1966) used conductive measurements to show that this reaction proceeds via the regenerative mechanism over wustite at 1,173 K. Wagner (1970) has reviewed several of these studies, and he has also discussed the equations which relate the rates of catalyst oxidation and reduction to experimentally observable parameters. In the present discussion, these equations will be briefly introduced and applied to gravimetric studies of reactions (Eqs. 1 and 2) on magnetite.

At equilibrium for reactions (Eqs. 1 and 2), the thermodynamic activity of oxygen-containing surface sites,  $a_{\text{O}^*}$ , divided by the activity of vacant surface sites,  $a_*$ , is given by:

$$\left(\frac{a_{\text{O}^*}}{a_*}\right)_e = K_{\text{CO}_2} \left(\frac{P_{\text{CO}_2}}{P_{\text{CO}}}\right) = K_{\text{CO}_2} \left(K_{\text{WGS}} \frac{P_{\text{H}_2\text{O}}}{P_{\text{H}_2}}\right) \quad (3)$$

where the subscript  $e$  refers to the equilibrium value of the activity ratio and  $K_{\text{CO}_2}$  is the equilibrium constant for the reverse of reaction (1). At a given temperature, the equilibrium ratio of surface activities is a function of the  $P_{\text{CO}_2}/P_{\text{CO}}$  or  $P_{\text{H}_2\text{O}}/P_{\text{H}_2}$  ratios of the gas phase. Each partial pressure ratio, therefore, defines a unique, equilibrium ratio of surface oxygen-site to vacant-site activities.

Near equilibrium, the net rate of either reaction (1) or the reverse of reaction (2) may be written as:

$$\frac{1}{S} \frac{dX}{dt} = r_e \left(\frac{-\Delta G}{RT}\right) \quad (4)$$

where  $X$  is the extent of surface oxygen removal from the catalyst and  $r_e$  is absolute rate of the forward and reverse reactions at equilibrium (i.e., the equilibrium exchange rate). In terms of the present gravimetric measurements,

$$X = n^0 - n \quad (5)$$

where  $n^0$  is the number of oxygen-containing surface sites for a chosen reference state (i.e.,  $P_{\text{CO}_2}/P_{\text{CO}} = 10.8$ ) and  $n$  is the time-dependent number of surface oxygen-containing sites during studies of reactions (Eqs. 1 or 2) at different  $P_{\text{CO}_2}/P_{\text{CO}}$  or  $P_{\text{H}_2\text{O}}/P_{\text{H}_2}$  ratios. In short, such studies are carried out by perturbing the catalyst away from equilibrium and monitoring the relaxation (i.e., change in weight) of the catalyst to the equilibrium state defined by the  $P_{\text{CO}_2}/P_{\text{CO}}$  or  $P_{\text{H}_2\text{O}}/P_{\text{H}_2}$  gas phase ratio. If the number of gaseous species is much greater than the number of surface sites, then the gas phase composition does not change significantly during such measurements and  $\Delta G$  can be related to the activities of surface species only:

$$\frac{-\Delta G}{RT} = \ell n \left\{ \frac{a_{\text{O}^*}/a_*}{(a_{\text{O}^*}/a_*)_e} \right\} \quad (6)$$

where  $a_{\text{O}^*}/a_*$  is the ratio of surface oxygen-site to vacant-site activities at time  $t$  after commencement of reaction. In general  $\ell n(a_{\text{O}^*}/a_*)$  depends on  $X$ , and near equilibrium this dependence can be expressed by the first terms of a Taylor series:

$$\ell n(a_{\text{O}^*}/a_*) = \ell n(a_{\text{O}^*}/a_*)_e + \left(\frac{d}{dX} \ell n(a_{\text{O}^*}/a_*)\right)_{X_e} (X - X_e) \quad (7)$$

where  $X_e$  is the extent of surface oxygen removal (relative to the reference state) at the equilibrium defined by the gas phase. Combining Eqs. 4-7 and integrating yields the following result:

$$\frac{n - n_e}{n^0 - n_e} = \exp \left\{ S r_e \left[ \frac{d}{dX} \ell n(a_{\text{O}^*}/a_*) \right]_{X_e} t \right\} \quad (8)$$

where  $n_e$  is the number oxygen-containing surface sites of the equilibrium defined by the gas phase. Since changes in  $n$  (i.e.,  $n - n_e$ ,  $n^0 - n$ ) can be determined gravimetrically, it is possible to determine the product of  $r_e$  and  $[d/dX \ell n(a_{\text{O}^*}/a_*)]_{X_e}$  from experimental data. Furthermore, since the latter term can be determined from equilibrium data, it is now possible to calculate  $r_e$  from Eq. 8 and time-dependent gravimetric data.

The implementation of the above strategy is summarized in Figure 1. In short, perturbations of catalyst temperature and gas phase partial pressure ratios are used to determine  $r_e$  and  $[d/dX \ell n(a_{\text{O}^*}/a_*)]_{X_e}$ , respectively. For determination of the latter, the equilibrium value of  $X$  has been measured at different  $P_{\text{CO}_2}/P_{\text{CO}}$  and  $P_{\text{H}_2\text{O}}/P_{\text{H}_2}$  gas ratios; and, since these gas phase ratios define  $(a_{\text{O}^*}/a_*)_e$  at equilibrium, it is possible to plot  $(a_{\text{O}^*}/a_*)$  versus  $X_e$  for each equilibrium state studied. A graphical evaluation of  $[d/dX \ell n(a_{\text{O}^*}/a_*)]_{X_e}$  is then possible. For determination of  $r_e$ , the response of the catalyst weight (and thus  $n - n_e$  or  $n^0 - n$ ) to temperature perturbations has been monitored at different  $P_{\text{CO}_2}/P_{\text{CO}}$  and  $P_{\text{H}_2\text{O}}/P_{\text{H}_2}$  gas ratios; and, it is thereby possible, through use of Eq. 8, to calculate the product of  $r_e$  and  $[d/dX \ell n(a_{\text{O}^*}/a_*)]_{X_e}$  for the various conditions studied. Combined

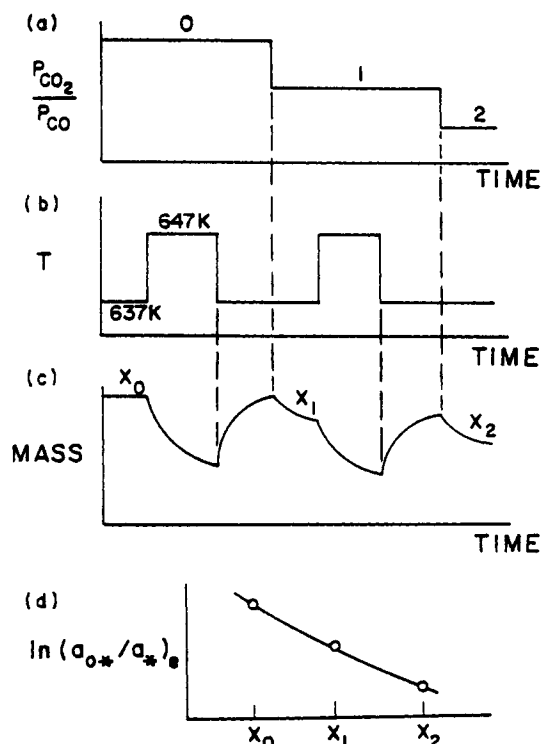


**Figure 1.** Experimental strategies employed in equilibrium and kinetic studies of oxygen removal from magnetite. (a)  $P_{\text{CO}_2}/P_{\text{CO}}$  (or  $P_{\text{H}_2\text{O}}/P_{\text{H}_2}$ ) ratio of the gas phase as a function of time. (b) Furnace temperature as a function of time. (c) Response of catalyst weight to step changes in  $P_{\text{CO}_2}/P_{\text{CO}}$  and  $T$ . (d) Correlation between activity ratio,  $(a_{\text{O}_2}/a_{*})_e$  (defined by Eq. 3) and extent of surface oxygen removal. Plot (d) is generated by cross-plotting the equilibrium measurements of curves (a) and (c).

with those measurements of  $[d/dX \ln(a_{\text{O}_2}/a_{*})]_{X_e}$ , it is then possible to determine  $r_e$  as a function of  $X$ .

#### Procedures for Data Collection

The catalyst used in this study was a commercial, high-temperature water-gas shift catalyst obtained from Haldor Topsøe A/S (SK 12). The catalyst is chromia promoted iron oxide (ca. 7%  $\text{Cr}_2\text{O}_3$ ) with a surface area of ca.  $40 \text{ m}^2/\text{g}$ . Approximately 200 mg of the catalyst was suspended from a Cahn RG microbalance. The catalyst was initially reduced to its active magnetite state by treatment for 24 h at 653 K in a static  $\text{CO}_2/\text{CO}$  gas mixture ( $P_{\text{CO}_2}/P_{\text{CO}} = 5.67$ ; total pressure = 26.7 kPa). After reduction, the sample was evacuated for 1 h at 653 K (final pressure =  $10^{-3}$  Pa). A gas mixture with  $P_{\text{CO}_2}/P_{\text{CO}} = 31.1$  was then dosed into the reaction chamber and the catalyst was allowed to equilibrate for 15 h at 637 K. This  $\text{CO}_2/\text{CO}$  mixture then formed the reference state for all subsequent experiments, with extents of oxygen removal measured with respect to the equilibrium surface oxygen content defined by this mixture. From this starting point, changes in the  $\text{CO}_2/\text{CO}$  gas ratio were achieved by pulsing into the reaction chamber either pure CO or  $\text{CO}_2$ . Since the volume of the reaction chamber was large (ca.  $4 \text{ dm}^3$ ), a recirculating bellows pump (Metal Bellows Corp., model MB-41) was used to mix the gaseous contents of the chamber after each gas phase pulse. The catalyst weight was allowed to equilibrate and the weight change which accompanied the change in  $\text{CO}_2/\text{CO}$  ratio was noted. After appropriate corrections for buoyancy and adsorption effects (the latter to be discussed later), these mass changes for different  $P_{\text{CO}_2}/P_{\text{CO}}$  ratios allow  $X$  (defined by Eq. 5) to be determined as a function of the ratio of surface oxygen-site to vacant-site activities (defined by Eq. 3). From these data,  $[d/dX \ln(a_{\text{O}_2}/a_{*})]_{X_e}$  was then calculated at different values of  $X$ . At each new equilibrium weight for a given  $P_{\text{CO}_2}/P_{\text{CO}}$  ratio, the sample temperature was then perturbed by 10 K. The time dependence of the sample weight which accompanied the temperature decrease from 647 K to 637 K was used, in conjunction

with Eq. 8 to calculate  $r_e$ . A similar strategy was employed for the  $\text{H}_2\text{O}/\text{H}_2$  system, although in this case only  $\text{H}_2$  pulses were used in changing the  $\text{H}_2\text{O}/\text{H}_2$  ratio. For both the  $\text{CO}_2/\text{CO}$  and the  $\text{H}_2\text{O}/\text{H}_2$  systems, gas ratios were chosen such that  $\text{Fe}_3\text{O}_4$  was the thermodynamically stable phase of iron at 637 K. Surface area measurements were performed on the catalyst before and after the  $\text{CO}_2/\text{CO}$  and  $\text{H}_2\text{O}/\text{H}_2$  studies to insure that the surface area remained constant during the course of all measurements. These BET isotherms were performed on the microbalance system using  $\text{N}_2$  at 77 K.

Carbon monoxide and  $\text{CO}_2$  were purified according to procedures described elsewhere (Kubsh et al., 1981), and stored in  $5 \text{ dm}^3$  bulbs. The  $\text{H}_2\text{O}/\text{H}_2$  gas mixture were prepared by passing  $\text{H}_2$  through a Deoxo unit followed by a  $\text{H}_2\text{O}$  bubbler. The  $\text{H}_2\text{O}/\text{H}_2$  ratio was controlled by adjusting the temperature of the bubbler to give the desired  $\text{H}_2\text{O}$  vapor pressure.

The microbalance system used in this study consists of a Cahn RG microbalance which has been incorporated into a conventional, diffusion-pumped vacuum system (ultimate system pressure of  $10^{-4}$  Pa). The microbalance has a short term sensitivity of  $2 \mu\text{g}$ , which allowed changes in the catalyst oxygen content of 0.001 monolayers to be measured for the 200 mg sample. The system contains a quadrupole mass spectrometer (UTI model 100°C) to monitor gas phase purity or the composition of gas mixtures. A Wallace and Teirnan differential pressure gauge (series 1000) is connected to the microbalance chamber and was used for all pressure measurements in the range 0.1–100 kPa. An Alpha model 4800 electromagnet may be moved into position around the sample and used in conjunction with the microbalance to measure the magnetic susceptibility of the catalyst (by the Faraday method). A maximum field of 6.1 kOe is attainable at the sample position with the electromagnet.

#### RESULTS

Before the changes of catalyst weight with temperature perturbations or changes in the gas phase partial pressure ratios can be used to study reactions (1) and (2), two other phenomena must be investigated: (i) the response of the catalyst temperature to the imposed perturbation in temperature of the furnace surrounding the sample; and (ii) the change in the extent of adsorption by CO and  $\text{CO}_2$  when the partial pressures of CO and  $\text{CO}_2$  are changed. With respect to the former phenomenon, the time constant for the catalyst thermal response was determined using *in situ* magnetization measurements. For these experiments a 20 mg sample of the catalyst was suspended from the microbalance in a  $\text{CO}_2/\text{CO}$  gas mixture ( $P_{\text{CO}_2}/P_{\text{CO}} = 5.67$ ) at a pressure of 26 kPa. For step changes in temperature between 637 K and 647 K, the magnetization of the sample responded quickly, indicating that thermal equilibrium was established within about 3 minutes.

With respect to adsorption phenomena, it is necessary to note that while the ratio of partial pressures determines the extent of oxygen removal from the surface ( $X$ ), the absolute partial pressures of gaseous species determine the extent of adsorption by CO,  $\text{CO}_2$ ,  $\text{H}_2\text{O}$  and  $\text{H}_2$ . In the study of different  $\text{H}_2\text{O}/\text{H}_2$  gas mixtures, the  $\text{H}_2\text{O}$  partial pressure was held constant while  $\text{H}_2$  was pulsed into the microbalance chamber. Accordingly, the extent of adsorption by  $\text{H}_2\text{O}$  can be assumed to be constant, and since the mass of  $\text{H}_2$  is much less than that of any oxygen-containing species, the weight changes due to changes in the extent of  $\text{H}_2$  adsorption can be neglected in studies of reaction (2). In fact, the surface coverage by  $\text{H}_2$  is expected to be small (Rachkovskii and Boreskov, 1970). This leaves one to account for changes in the extents of CO and  $\text{CO}_2$  adsorption during studies of reaction (1) in different  $\text{CO}_2/\text{CO}$  gas mixtures. Indeed, it has been shown elsewhere (Kubsh et al., 1981) that CO and  $\text{CO}_2$  do, in fact, adsorb to appreciable extents on magnetite under the conditions used in the present study. The corresponding mass changes due to adsorption of these species can be determined by pulsing into the microbalance chamber a gas mixture with a constant  $\text{CO}_2/\text{CO}$  composition. With a constant

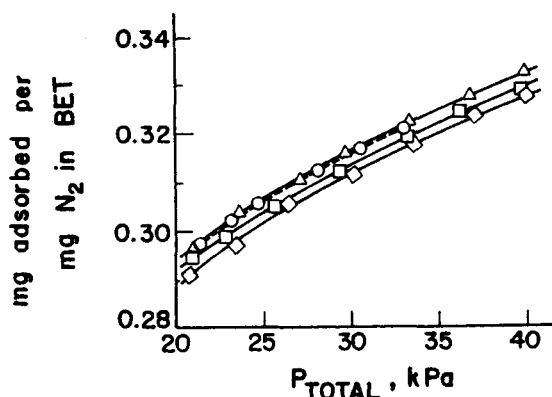


Figure 2. Total  $\text{CO}_2/\text{CO}$  adsorption uptakes of chromia-promoted magnetite at 637 K and different  $P_{\text{CO}_2}/P_{\text{CO}}$  ratios [ $P_{\text{CO}_2}/P_{\text{CO}} = 30$  ( $\square$ ), 10 ( $\Delta$ ), 2 ( $\diamond$ )]. Circles are actual equilibrium conditions encountered during  $\text{CO}_2$  pulses into a  $\text{CO}_2/\text{CO}$  gas mixture.

$P_{\text{CO}_2}/P_{\text{CO}}$  ratio the extent of oxygen removal from the catalyst ( $X$ ) is constant, but as the total pressure is increased the extents of adsorption by  $\text{CO}_2$  and  $\text{CO}$  increase. Figure 2 shows these adsorption isotherms, determined gravimetrically, at 637 K for  $P_{\text{CO}_2}/P_{\text{CO}}$  ratios of 30, 10, and 2. These weight changes are plotted versus total pressure as mg adsorbed per mg of  $\text{N}_2$  in the BET monolayer. At a given total pressure, the isotherms of Figure 2 show an apparent maximum in the weight of adsorbed species with respect to the  $P_{\text{CO}_2}/P_{\text{CO}}$  ratio. Analogous volumetric adsorption studies, reported elsewhere (Kubsh et al., 1981), indicate this apparent maximum is an artifact due to small errors associated with determining the weight of the catalyst in vacuum prior to collection of each isotherm. However, this uncertainty is not significant in the present study of reaction (1), as shown in Figure 2 for the conditions employed during  $\text{CO}_2$  pulsing into a  $\text{CO}_2/\text{CO}$  gas mixture. It can be seen therein that changes in the weight of adsorbed species due to changes in total pressure (given directly in the Figure) are more important than weight changes associated with variations in the  $P_{\text{CO}_2}/P_{\text{CO}}$  ratio (given by interpolation between isotherms). In addition to these equilibrium data, the time response of the catalyst weight to the above changes in total pressure (at constant  $P_{\text{CO}_2}/P_{\text{CO}}$ ) was also recorded. It was thereby noted that the catalyst weight reached a constant value within 3 minutes after changing the total pressure (for pressures greater than ca. 13 kPa).

As explained in the previous section, changes in catalyst weight were induced by: (i) pulsing  $\text{CO}$  or  $\text{CO}_2$  into  $\text{CO}_2/\text{CO}$  gas mixtures; and (ii) pulsing  $\text{H}_2$  into  $\text{H}_2\text{O}/\text{H}_2$ . With the results of Figure 2, those weight changes in  $\text{CO}_2/\text{CO}$  due to adsorption effects can be calculated and used to determine  $X$  from the experimental data. The weight changes observed in  $\text{H}_2\text{O}/\text{H}_2$  can be used to determine  $X$  without correction for adsorption effects. To make the data independent of sample size, the extent of oxygen removal ( $X$ ) is normalized by the number of  $\text{N}_2$  molecules in the BET monolayer for the sample, and this ratio is denoted by  $\theta_x$ . Figure 3 shows how  $\theta_x$  varies with  $a_{\text{O}_2}/a_*$ , the latter calculated from the  $P_{\text{CO}_2}/P_{\text{CO}}$  and  $P_{\text{H}_2\text{O}}/P_{\text{H}_2}$  ratios using Eq. 3. The slope of this semi-log plot is used to determine  $[d/dx \ln(a_{\text{O}_2}/a_*)]_{X_e}$ . The constant  $K_{\text{CO}_2}$  which appears in Eq. 3 is simply an additive factor to  $\ln(a_{\text{O}_2}/a_*)$  in such a semi-log plot, and it has no influence on the calculated slope. It has therefore been arbitrarily set equal to unity. The values of  $\theta_x$  in Figure 3 have all been referenced to a surface for which  $(a_{\text{O}_2}/a_*)$  equals 10.8 (i.e.,  $\theta_x = 0$  at  $a_{\text{O}_2}/a_* = 10.8$ ).

According to Eq. 8, the change in catalyst weight due to oxygen removal from the surface should depend exponentially on time,  $t$ , following thermal perturbation to a new equilibrium state. However, since the thermal response of the catalyst and adsorption effects occur during the first three minutes following the temperature perturbation (of the furnace surrounding the sample), those weight changes due to reactions (1) or (2) can only be readily studied at longer times. This is shown in Figure 4, which is a typical semilog plot of the catalyst weight change,  $m_e - m_t$  (equilibrium weight minus weight at time  $t$ ) vs.  $t$  after temperature perturbation

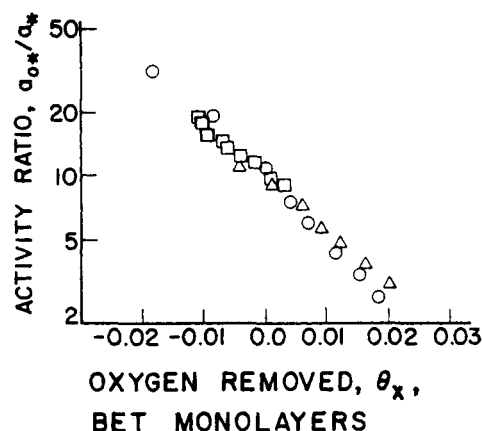


Figure 3. Activity ratio,  $a_{\text{O}_2}/a_*$  (as defined by Eq. 3), vs. the extent of surface oxygen removal from chromia promoted magnetite at 637 K.  $\circ$ ,  $\square$ , and  $\Delta$  are data acquired from  $\text{CO}$ ,  $\text{CO}_2$ , and  $\text{H}_2$  steps, respectively.  $\theta_x$  is defined to be zero at the reference state,  $P_{\text{CO}_2}/P_{\text{CO}} = 10.8$ .

from 647 to 637 K. Indeed for times longer than ca. 240 s, a good straight-line plot is obtained. While this plot was obtained at a given  $P_{\text{CO}_2}/P_{\text{CO}}$  ratio (equal to 13.5), a corresponding plot was obtained at a given  $P_{\text{CO}_2}/P_{\text{CO}}$  ratio (equal to 13.5), a corresponding plot was obtained for each of the points shown in Figure 3. From the slopes of the linear portions of these semilog plots it is possible to determine the corresponding products of  $r_e$  and  $[d/dx \ln(a_{\text{O}_2}/a_*)]_{X_e}$  using Eq. 8 and noting that  $m_f - m_t$  is proportional to  $(n - n_e)/(n^0 - n_e)$ . Since the value of  $d/dx \ln(a_{\text{O}_2}/a_*)$  can be obtained from the slope in Figure 3, it is now possible to calculate  $r_e$  (per unit surface area) for each of the points shown in this Figure. These data are summarized in Table 1.

From these values of  $r_e$  at different  $P_{\text{CO}_2}/P_{\text{CO}}$  and  $P_{\text{H}_2\text{O}}/P_{\text{H}_2}$  ratios, the rate constants of reactions (1) and (2) can be determined. Since  $r_e$  is an exchange rate it is equal to the forward and reverse rate of the particular reaction in question at equilibrium. If reactions (1) and (2) are mechanistic steps, the rate expressions for the forward and reverse directions may be written as:

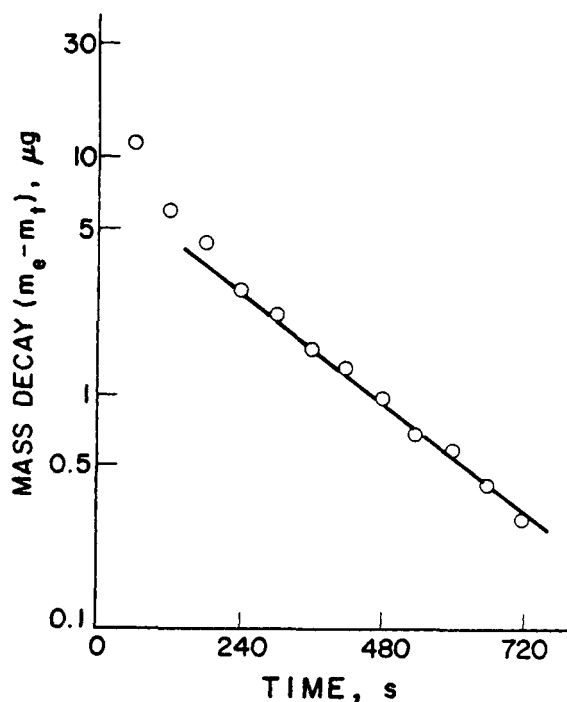


Figure 4. Weight change of chromia promoted magnetite after a step change in temperature from 647 to 637 K in a  $\text{CO}_2/\text{CO}$  atmosphere ( $P_{\text{CO}_2}/P_{\text{CO}} = 13.5$ ).

TABLE 1. EXPERIMENTALLY MEASURED EQUILIBRIUM EXCHANGE RATES ( $r_e$ )

Data from CO Steps			Data from CO <sub>2</sub> Steps			Data from H <sub>2</sub> Steps		
$P_{CO}$ (kPa)	$P_{CO_2}$ (kPa)	$r_e \times 10^{-14}$ (m <sup>-2</sup> s <sup>-1</sup> )	$P_{CO}$ (kPa)	$P_{CO_2}$ (kPa)	$r_e \times 10^{-14}$ (m <sup>-2</sup> s <sup>-1</sup> )	$P_{H_2}$ (kPa)	$P_{H_2O}$ (kPa)	$r_e \times 10^{-15}$ m <sup>-2</sup> s <sup>-1</sup> )
1.80	19.4	3.30	1.99	19.3	3.10	4.16	2.18	0.92
3.26	19.4	3.63	1.99	21.2	3.24	5.24	2.18	1.08
4.45	19.4	4.10	1.99	22.7	3.50	6.61	2.18	1.12
5.68	19.4	4.40	1.99	24.5	3.63	7.93	2.18	1.19
7.25	19.4	4.50	1.99	26.8	3.83	9.96	2.18	1.23
			1.99	28.6	3.96	11.8	2.18	1.30
			1.99	31.0	4.26			

TABLE 2. SUMMARY OF KINETIC PARAMETERS

	$k_{CO}$ (m/s)	$k_{CO_2}$ (m/s)	$k_{H_2}$ (m/s)	$k_{H_2O}$ (m/s)	$\theta_{0*}^{sat}$	$\theta_X^0$
CO Pulses	$5.6 \times 10^{-8}$	$3.2 \times 10^{-9}$	—	—	0.082	0.049
CO <sub>2</sub> Pulses	$4.7 \times 10^{-8}$	$2.1 \times 10^{-9}$	—	—	0.092	0.058
H <sub>2</sub> Pulses	—	—	$5.5 \times 10^{-8}$	$7.0 \times 10^{-8}$	0.086	0.050
Average	$5.2 \times 10^{-8}$	$2.6 \times 10^{-9}$	$5.5 \times 10^{-8}$	$7.0 \times 10^{-8}$	0.087	0.052

$$r_e = r_i = k_i P_i \theta_{0*} \quad i = \text{CO or H}_2 \quad (9)$$

$$r_e = r_i = k_i P_i \theta_* \quad i = \text{CO}_2 \text{ or H}_2\text{O} \quad (10)$$

where all rates  $r_i$  are per unit surface area. In terms of the experimentally measurable extent of oxygen removal,  $\theta_X$ , the following expressions for  $\theta_*$  and  $\theta_{0*}$  may be defined:

$$\theta_* = \theta_X + \theta_X^0 \quad (11)$$

$$\theta_{0*} = \theta_{0*}^{sat} - \theta_* = \theta_{0*}^{sat} - \theta_X^0 - \theta_X \quad (12)$$

where  $\theta_X^0$  is the fraction of the BET monolayer consisting of vacant sites at the reference state (for which  $a_{0*}/a_* = 10.8$ ), and  $\theta_{0*}^{sat}$  is the fraction of the BET monolayer consisting of oxygen-containing sites when all of the vacant sites have been saturated by oxygen (i.e.,  $\theta_* = 0$ ). Substitution for  $\theta_{0*}$  and  $\theta_*$ , using Eqs. 11 and 12, in Eqs. 9 and 10 results in a set of equations relating  $r_e$  to  $\theta_X$ :

$$\frac{r_e}{P_i} = k_i (\theta_{0*}^{sat} - \theta_X^0) - k_i \theta_X \quad i = \text{CO or H}_2 \quad (13)$$

$$\frac{r_e}{P_i} = k_i \theta_X^0 + k_i \theta_X \quad i = \text{CO}_2 \text{ or H}_2\text{O} \quad (14)$$

In short, plots of  $r_e/P_i$  vs.  $\theta_X$  should be linear, with slopes equal to  $\pm k_i$ . Dividing the intercepts of these plots by  $k_i$  should equal  $\theta_{0*}^{sat} - \theta_X^0$  in the case of  $i = \text{CO, H}_2$  or should equal  $\theta_X^0$  in the case of  $i =$

CO<sub>2</sub>, H<sub>2</sub>O. Figures 5 and 6 depict these plots of  $r_e/P_i$  vs.  $\theta_X$  for the three sequences of experiments performed in this study (i.e., pulsing with CO, CO<sub>2</sub> or H<sub>2</sub>) and all plots exhibit the linear behavior predicted by Eqs. 13 and 14. Table 2 summarizes the values of the four rate constants,  $\theta_X^0$ , and  $\theta_{0*}^{sat}$  obtained from the slopes and intercepts of Figures 5 and 6.

## DISCUSSION

Before discussing the regenerative mechanism and water-gas shift over magnetite, it may be questioned whether the gravimetric measurements of the present study actually reflect oxygen removal from the surface, in contrast to oxygen removal from the bulk. For example, as shown by Kasatkina et al. (1973), the oxygen in CO or CO<sub>2</sub> can exchange at 600 K with lattice oxygen below the surface of magnetite. In CO and CO<sub>2</sub> adsorption studies reported elsewhere (Kubsh et al., 1981), however, it has been shown that the surface coverages by carbon monoxide,  $\theta_{CO}$ , and carbon dioxide,  $\theta_{CO_2}$ , can be correlated with the presently, gravimetrically measured value of  $\theta_X$  (assuming that oxygen removal is from the surface only). Specifically, for a given increase in  $\theta_X$ , there is a corresponding

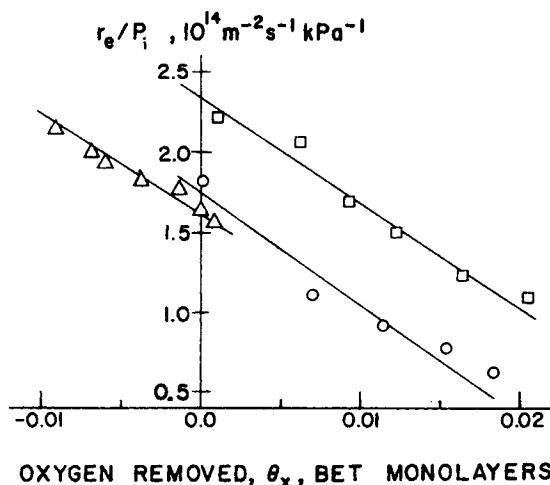


Figure 5.  $r_e/P_i$  versus extent of surface oxygen removal at 637 K.  $\circ$  are data acquired from CO steps with  $P_{CO_2}$  constant at 19.4 kPa ( $i = \text{CO}$ ).  $\Delta$  are data acquired from CO<sub>2</sub> steps with  $P_{CO}$  constant at 1.99 kPa ( $i = \text{CO}$ ).  $\square$  are data acquired from H<sub>2</sub> steps with  $P_{H_2O}$  constant at 2.18 kPa ( $i = \text{H}_2$ ).

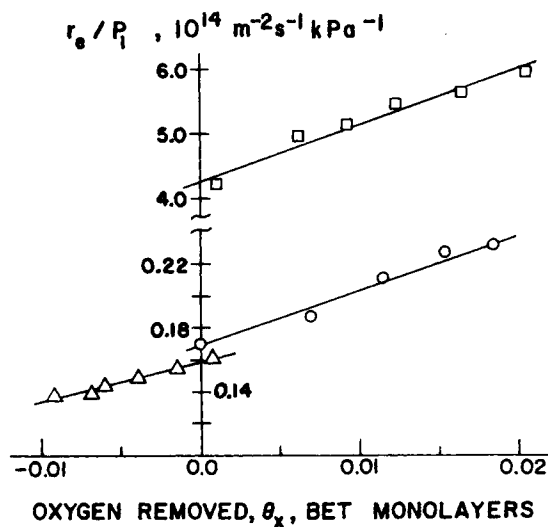


Figure 6.  $r_e/P_i$  vs. extent of surface oxygen removal at 637 K.  $\circ$  are data acquired from CO steps with  $P_{CO_2}$  constant at 19.4 kPa ( $i = \text{CO}_2$ ).  $\Delta$  are data acquired from CO<sub>2</sub> steps with  $P_{CO}$  constant at 1.99 kPa ( $i = \text{CO}_2$ ).  $\square$  are data acquired from H<sub>2</sub> steps with  $P_{H_2O}$  constant at 2.18 kPa ( $i = \text{H}_2\text{O}$ ).

increase in  $\theta_{\text{CO}}$  and a corresponding decrease in  $\theta_{\text{CO}_2}$ . This supports the assumption that gravimetric measurements of this study can be used to determine changes in the amount of oxygen on the surface of magnetite.

From the results of the present equilibrium and kinetic relaxation studies of reactions (1) and (2), it is possible to test whether these two steps form a valid mechanism, and further an important pathway, for water-gas shift over magnetite. Consider first the determinations of the equilibrium surface coverages by  $\text{O}^*$  and  $*$  (Figure 3 and Table 2). According to reactions (1) and (2) the equilibrium surface coverage by  $\text{O}^*$  in  $\text{CO}_2/\text{CO}$  or  $\text{H}_2\text{O}/\text{H}_2$  gas mixtures should be dependent only on  $a_{\text{O}^*}/a_*$ , as given by Eq. 3 and either  $P_{\text{CO}_2}/P_{\text{CO}}$  or  $P_{\text{H}_2\text{O}}/P_{\text{H}_2}$ . The data of Figure 3 indicate that the equilibrium extent of oxygen removal from the catalyst (and thus  $\theta_{\text{O}^*}$ ) is, in fact, equivalent in  $P_{\text{CO}_2}/P_{\text{CO}}$  and  $P_{\text{H}_2\text{O}}/P_{\text{H}_2}$  ratios corresponding to the same value of  $a_{\text{O}^*}/a_*$ . Furthermore, the data in  $\text{CO}_2/\text{CO}$  gas mixtures were collected using both  $\text{CO}$  and  $\text{CO}_2$  pulses; and, Figure 3 shows the equivalence of these data for the same  $P_{\text{CO}_2}/P_{\text{CO}}$  ratio but at different total pressures. This provides support for the prediction that the equilibrium surface coverage by  $\text{O}^*$  depends on ratios of partial pressures and not on the absolute values of individual partial pressures. It can also be noted in Figure 3 that the range of  $a_{\text{O}^*}/a_*$  ratios studied in the present work apparently creates only small extents of oxygen removal from the catalyst: (i.e., changes in  $\theta_X$  of the order of 0.01). However, the saturation coverage of the surface by oxygen  $\theta_{\text{O}^*}^{\text{sat}}$  is approximately 9% of the BET monolayer, as determined from the slopes and intercepts of Figures 5 and 6. Thus the range of  $\theta_X$  investigated in this study is appreciable, corresponding to approximately 35% of the total available oxygen on the surface at saturation (i.e., when  $\theta_* = 0$ ). In summary, the equilibrium behavior of oxygen at the surface of magnetite in  $\text{CO}_2/\text{CO}$  and  $\text{H}_2\text{O}/\text{H}_2$  gas mixtures is adequately described by reactions (1) and (2), the two steps of the regenerative mechanism.

Consider next the kinetics of reactions (1) and (2). The straight-line plots of Figures 5 and 6 verify the utility of Eqs. 9 and 10 in describing the kinetics of these two reactions. In addition, for thermodynamic consistency, the corresponding rate constants defined by Eqs. 9 and 10 must satisfy:

$$\frac{k_{\text{CO}}k_{\text{H}_2\text{O}}}{k_{\text{CO}_2}k_{\text{H}_2}} = K_{\text{WGS}} \quad (15)$$

The ratio of rate constants determined experimentally at 637 K is equal to 25.4, compared to the value of 17.6 for  $K_{\text{WGS}}$  at this temperature. This agreement seems acceptable, especially since the calculation of these four rate constants from Figures 5 and 6 did not involve any assumption regarding the value of  $K_{\text{WGS}}$ .

While the above arguments reflect the validity of reactions (1) and (2) in describing the thermodynamics and kinetics of oxygen removal from (or incorporation into) the surface of magnetite, the importance of the regenerative mechanism as a water-gas shift pathway must be ascertained. This is done by using the results of Table 2 to predict the overall rate and the form of the rate expression for water-gas shift, and then comparing these predictions with actual studies of water-gas shift kinetics over magnetite. By analogy with the derivation of Temkin (1976), the regenerative mechanism over a uniform surface (described by Eqs. 9 and 10) gives rise to the following expression for the forward rate of water-gas shift,  $r_{\text{WGS}}$ :

$$r_{\text{WGS}} = \frac{k_{\text{CO}}k_{\text{CO}_2}\theta_{\text{O}^*}^{\text{sat}}P_{\text{CO}}P_{\text{H}_2\text{O}}}{k_{\text{CO}}P_{\text{CO}} + k_{\text{H}_2\text{O}}P_{\text{H}_2\text{O}} + k_{\text{CO}_2}P_{\text{CO}_2} + k_{\text{H}_2}P_{\text{H}_2}} \quad (16)$$

Reaction rates predicted from this expression and Table 2 can be compared with water-gas shift rates measured experimentally by Bohlbro (1969) on a chromia-promoted magnetite catalyst similar to the one used in the present study. In particular, the kinetic data collected by Bohlbro were fit to a power law, that at 637 K has the form:

$$r_{\text{WGS}} = 2.0 \times 10^{15} \frac{P_{\text{CO}}^{0.9} P_{\text{H}_2\text{O}}^{0.25}}{P_{\text{CO}_2}^{0.6}} \quad (17)$$

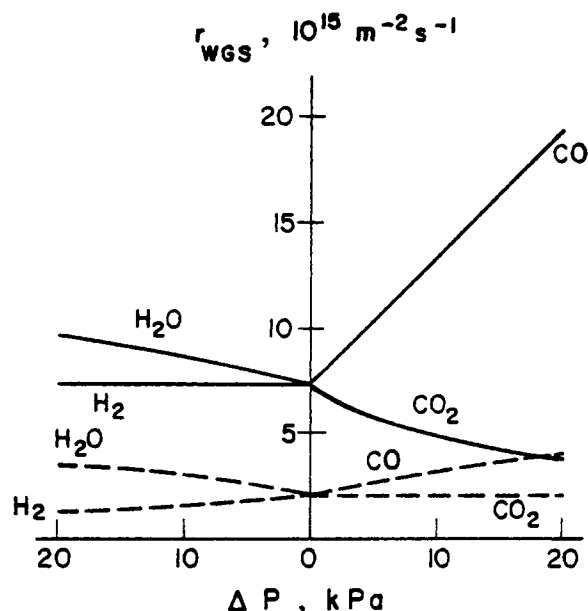


Figure 7. The net forward rate of water-gas shift,  $r_{\text{WGS}}$ , at 637 K as predicted by the kinetic parameters of Table 2 (dashed lines), and compared to  $r_{\text{WGS}}$  calculated from Bohlbro's power law rate expression (solid lines). The effect of individually increasing the partial pressure of each component from 10 kPa to 30 kPa is given by  $\Delta P$  ( $\Delta P = 0$  corresponds to all  $P_i = 10$  kPa).

where  $r_{\text{WGS}}$  and  $P_i$  are in units of  $\text{m}^{-2} \text{s}^{-1}$  and kPa, respectively. As a basis for comparison all  $P_i$  are set equal to 10 kPa, a pressure typical of those used in the present study and in the study of Bohlbro. Equation 16 predicts a rate of  $2.1 \times 10^{15} \text{ m}^{-2} \text{s}^{-1}$ , and the measured rate given by Eq. 17 is equal to  $7.3 \times 10^{15} \text{ m}^{-2} \text{s}^{-1}$ . The agreement between these two values is good. The partial pressure dependence of these two expressions is shown in Figure 7, where the effects of increasing each of the partial pressures from 10 kPa to 30 kPa can be seen. Qualitatively, the dependence of  $r_{\text{WGS}}$  on  $P_{\text{CO}}$ ,  $P_{\text{CO}_2}$  and  $P_{\text{H}_2\text{O}}$  is similar for the two rate expressions:  $r_{\text{WGS}}$  increases with increasing  $P_{\text{CO}}$  and  $P_{\text{H}_2\text{O}}$ , and it decreases with increasing  $P_{\text{CO}_2}$ . Quantitatively, the dependence of  $r_{\text{WGS}}$  on  $P_{\text{CO}}$  and  $P_{\text{CO}_2}$  is stronger in the measured rate expression of Bohlbro than in the predicted rate expression of the present study. In addition, the predicted rate expression shows  $\text{H}_2$  to be an inhibitor of water-gas shift, while the measured rate of water-gas shift is independent of hydrogen pressure. In summary, the rate expression (Eq. 16) and rate constants (Table 2) for the regenerative mechanism are able to predict qualitatively both the rate of water-gas shift and its partial pressure dependence over magnetite. It is, therefore, suggested that the regenerative mechanism over magnetite is, in fact, an important pathway for water-gas shift. The quantitative aspects of this statement will be discussed below.

From the measurements of the present study it is not possible to determine the nature (e.g., coordination) of the active sites for the regenerative mechanism over magnetite. It can be concluded, however, that the number of such sites (i.e.,  $\theta_{\text{O}^*}^{\text{sat}}$ ) is only a small fraction of the total number of oxygen atoms (including lattice and adsorbed oxygen) present at the surface. Specifically, only 9% of the BET surface area is active in the regenerative pathway for water-gas shift. This may indicate that  $\text{O}^*$  must have a specific coordination or a unique electronic structure which allows it to precipitate in the oxidation-reduction sequence given by reactions (1) and (2). For example, preliminary ESCA studies on this chromia-promoted magnetite catalyst indicate that the surface is significantly enriched in chromium (compared to the 7% chromium-content of the bulk). Correspondingly, a large fraction of the oxygen atoms at the surface might have Cr-O linkages that alter the oxidation-reduction behavior required for the regenerative mechanism. It should be noted that it would perhaps be more correct to treat the surface of this catalyst as being non-uniform (i.e., with  $\text{O}^*$  sites having a distribution of catalytic activities). A

study by Shchibrya et al. (1965) found that water-gas shift kinetic data obtained on a chromia-promoted magnetite catalyst were best fit by the regenerative mechanism over a non-uniform surface. Over the range of  $\theta_X$  investigated in the present study, such surface non-uniformities were not detected (as shown by the straight-line plots in Figures 5 and 6). Hence, the present data are treated in terms of a small number of surface sites ( $\theta_{0*}^{\text{sat}}$ ) having a constant catalytic activity. This assumption, however, may be one source of the quantitative differences between that water-gas shift rate expression predicted in the present study and that measured by Bohlbro.

Another complication in the quantitative use of reactions (1) and (2) to describe water-gas shift over magnetite is the presence of adsorbed species other than  $0*$ , as mentioned previously (e.g., adsorption of CO and  $\text{CO}_2$ ). In work described elsewhere (Kubsh et al., 1981), it has been shown that CO and  $\text{CO}_2$  adsorb on chromia-promoted magnetite to a significant extent under those conditions used in the present study. In particular, surface coverages by CO and  $\text{CO}_2$  ( $\theta_{\text{CO}}$  and  $\theta_{\text{CO}_2}$ ) of the order of 10% and 15% of the BET monolayer, respectively, were measured. Furthermore, it was noted above that these coverages correlate with the amount of  $0*$  on the catalyst surface, the latter given by Figure 3. However,  $\theta_{\text{CO}_2}$  and  $\theta_{\text{CO}}$  also depend on the absolute values of  $P_{\text{CO}_2}$  and  $P_{\text{CO}}$  respectively, while the results of Figure 3 indicate that the equilibrium surface coverage by  $0*$  is dependent only on the ratio  $P_{\text{CO}_2}/P_{\text{CO}}$  or  $P_{\text{H}_2\text{O}}/P_{\text{H}_2}$ . This suggests that the presence of adsorbed CO and  $\text{CO}_2$  does not significantly alter  $\theta_{0*}$ , consistent with the regeneration mechanism described by reactions (1) and (2). In addition, it is shown elsewhere (Kubsh et al., 1981) that the CO and  $\text{CO}_2$  adsorption data can be correlated quantitatively using a model in which  $\theta_{\text{CO}}$  and/or  $\theta_{\text{CO}_2}$  do not compete with  $\theta_{0*}$  for the same vacant sites,  $*$ .

With the knowledge that CO and  $\text{CO}_2$  adsorb to a significant extent on magnetite at temperature typical of water-gas shift conditions, it is tempting to rewrite Eqs. 1 and 2 in terms of adsorbed reactants and products instead of gas phase (or weakly adsorbed) species. The regenerative mechanism for water-gas shift would then consist of these two modified reactions plus adsorption/desorption steps for CO,  $\text{CO}_2$ ,  $\text{H}_2\text{O}$  and  $\text{H}_2$ . Since it was shown in the results section that adsorption processes appear to be much faster than oxygen removal from (or incorporation into) the surface, the adsorption/desorption steps of this modified regenerative mechanism can be assumed to be in equilibrium. For such a model, plots of  $\tau_e/\theta_i$  versus  $\theta_X$  (analogous to the plots in Figures 5 and 6) should be linear, and the slopes should equal the rate constants for the modified forms of Eqs. 1 and 2. The data, however, do not conform to this prediction; and in contrast to the plots of Figures 5 and 6 which show good linear behavior, plots of  $\tau_e/\theta_i$  versus  $\theta_X$  show considerable curvature for  $i = \text{CO}, \text{CO}_2$ . It is thus suggested that gas phase, or weakly adsorbed, reactants and products are involved in the process of oxygen removal from (or incorporation into) the surface of magnetite, and this process can be adequately described by reactions (1) and (2).

Even though the kinetics of the regenerative mechanism appear to be unaffected by  $\theta_{\text{CO}}$  and  $\theta_{\text{CO}_2}$ , these adsorbed species may contribute to the overall rate of water-gas shift through an independent pathway. This second pathway may, in fact, proceed via an adsorptive mechanism, such as that proposed by Oki et al. (1972). The combination of regenerative and adsorption reaction pathways over magnetite may be the reason why this catalyst is particularly active for water-gas shift, as compared to other oxide catalysts in this temperature range. This may also explain the quantitative differences between the kinetics of water-gas shift predicted by the regenerative mechanism (Eq. 16) and those overall kinetics measured experimentally (Eq. 17).

#### ACKNOWLEDGMENTS

We wish to thank Prof. M. Boudart for stimulating discussions during the formative stages of this research work. We also ac-

knowledge the National Science Foundation (ENG 79-11130) for providing financial support for this research.

#### NOTATION

$a_{0*}$	= activity of $0*$ , oxygen-containing surface sites
$a_*$	= activity of $*$ , vacant surface sites
$\Delta G$	= Gibbs free energy change, $\text{kJ}\cdot\text{mol}^{-1}$
$k_i$	= rate constant, $\text{m}\cdot\text{s}^{-1}$
$K_i$	= equilibrium constants for reactions (1) and (2)
$K_{\text{WGS}}$	= equilibrium constant for the water-gas shift reaction
$m_e$	= catalyst weight at equilibrium (i.e., conclusion of the relaxation process), $\mu\text{g}$
$m_t$	= catalyst weight at time $t$ during the relaxation process, $\mu\text{g}$
$n$	= number of oxygen containing surface sites at time $t$ during relaxation measurements
$n^0$	= number of oxygen containing surface sites at the reference condition, $P_{\text{CO}_2}/P_{\text{CO}} = 10.8$
$n_e$	= number of oxygen containing surface sites at equilibrium
$P_i$	= partial pressure of competent $i$ , $\text{kPa}$
$r_e$	= equilibrium exchange reaction rate, $\text{m}^{-2}\cdot\text{s}^{-1}$
$r_i$	= reaction rate, $\text{m}^{-2}\cdot\text{s}^{-1}$
$r_{\text{WGS}}$	= net forward reaction rate of water-gas shift, $\text{m}^{-2}\cdot\text{s}^{-1}$
$R$	= gas constant
$S$	= catalyst surface area, $\text{m}^2$
$t$	= time, $\text{s}$
$T$	= temperature, $\text{K}$
$X$	= extent of surface oxygen removal (relative to the reference state defined by $P_{\text{CO}_2}/P_{\text{CO}} = 10.8$ ), atoms of oxygen
$X_e$	= extent of surface oxygen removal at equilibrium (relative to the reference state defined by $P_{\text{CO}_2}/P_{\text{CO}} = 10.8$ ), atoms of oxygen

#### Greek Letters

$\theta_{0*}$	= surface coverage of oxygen containing sites, BET monolayers
$\theta_*$	= surface coverage of vacant sites, BET monolayers
$\theta_X$	= extent of surface oxygen removal relative to the reference condition defined by $P_{\text{CO}_2}/P_{\text{CO}} = 10.8$ , BET monolayers
$\theta_X^0$	= extent of surface oxygen removal at the reference condition defined by $P_{\text{CO}_2}/P_{\text{CO}} = 10.8$ , BET monolayers
$\theta_{0*}^{\text{sat}}$	= coverage of oxygen containing sites at saturation (i.e., $0* = 0$ ), BET monolayers
$\theta_i$	= surface coverage of species $i$ , BET monolayers

#### LITERATURE CITED

- Bohlbro, H., "An Investigation on the Kinetics of the Conversion of Carbon Monoxide by Water Vapour over Iron Oxide Based Catalysts," Gjellerup, Copenhagen (1959).
- Boreskov, G. K., T. M. Yur'eva, and A. S. Sergeeva, "Mechanism of the Conversion of Carbon Monoxide on Iron-Chromium Catalyst," *Kinet. Katal.*, 11, 1476 (1970).
- Glavachek, V., M. Marek, and M. Korzhinkova, "Kinetics of the Catalytic Reaction of Carbon Monoxide with Water Vapor," *Kinet. Katal.*, 9, 1107 (1968).
- Grabke, H. J., and H. Viehhaus, "Surface Composition of Wustite," *Ber. Bunsenges. Phys. Chem.*, 84, 152 (1980).
- Happel, J., "Study of Kinetic Structure Using Marked Atoms," *Catal. Rev.*, 6, 221 (1972).
- Kaneko, Y., and S. Oki, "On the Mechanism of the Water-Gas Shift Reaction," *J. Res. Inst. Catal.*, Hokkaido Univ., 15, 185 (1967).
- Kasatkina, L. A., V. N. Mekipelov, and N. N. Zhivotenko, "The Isotope Exchange Reaction of Carbon Monoxide over  $\text{Fe}_3\text{O}_4$ ," *Kinet. Katal.*, 14, 363 (1973).
- Kubsh, J. E., Chen Yi, and J. A. Dumesic, "The Use of  $\text{CO}_2/\text{CO}$  Gas Mix-

- tures to Study Adsorption on Chromia-Promoted Magnetite at Water-Gas Shift Temperatures," accepted for publication in *J. Catal.* (1981).
- Kul'kova, N. V., and M. I. Temkin, "Kinetics of the Reaction of Conversion of Carbon Monoxide by Water Vapor," *Z. Fiz. Khim.*, **23**, 695 (1949).
- Oki, S., J. Happel, M. Hnatow, and Y. Kaneko, "The Mechanism of the Water-Gas Shift Reaction over Iron Oxide Catalyst," *Proc. Intern. Congr. Catal.*, No. 5, 173 (1973).
- , and R. Mezaki, "Identification of Rate-Controlling Steps for the Water-Gas Shift Reaction Over an Iron Oxide Catalyst," *J. Phys. Chem.*, **77**, 447 (1973).
- Podolski, W. F., and Y. G. Kim, "Modeling the Water-Gas Shift Reaction," *Ind. Eng. Chem. Process Des. Develop.*, **13**, 415 (1974).
- Rachkovskii, E. E., and G. K. Boreskov, "The Mechanism of Isotope Exchange in the System  $H_2 - H_2O$  on Some Oxide Catalysts," *Kinet. Katal.*, **11**, 1410 (1970).
- Riecke, V. E., and K. Bohnenkamp, "On the Kinetics of Oxidation and Reduction of Wustite within its Range of Existence," *Arch. Eisenhütten*, **40**, 717 (1969).
- Shchibrya, G. G., N. M. Morozov, and M. I. Temkin, "The Kinetics and Mechanism of the Catalytic Reaction Between Carbon Monoxide and Steam," *Kinet. Katal.*, **6**, 1057 (1965).
- Stotz, V. S., "Investigations Concerning the Mechanism of the Water-Gas Shift Reaction on Wustite," *Ber. Bunsenges. Phys. Chem.*, **70**, 769 (1966).
- Temkin, M. I., "Relaxation Rate of a Two-Stage Catalytic Reaction," *Kinet. Katal.*, **17**, 1095 (1976).
- Wagner, E., "Adsorbed Atomic Species as Intermediates in Heterogeneous Catalysis," *Adv. in Catal.*, **21**, 323 (1970).

Manuscript received April 24, 1981; revision received September 16, and accepted October 13, 1981.

# Complex Transitional Flows in Concentric Annuli

Detailed measurements of radial variations of turbulence intensity were made with a hot film anemometer in a concentric annulus of aspect ratio  $R_i/R_o = 0.0416$  for a Reynolds number range  $1,200 \leq Re \leq 3,000$  using a Newtonian polyglycol water solution. Measurements were also made of excess entrance pressure gradients and the axial variation of pressure gradients.

Based on the results of these measurements, it is concluded that the proposition of Lea and Tadros (1931), Rothfus (1948) and others that a transitional flow regime develops with a zone of turbulence near the inner core surrounded by a zone of laminar flow near the outer wall is false. The two-critical Reynolds number transitional regime proposed by Hanks and Bonner (1971) is verified to exist but their mathematical model for the interpretation of its cause is disproved. It is shown that at the lower critical Reynolds number predicted by Hanks and Bonner (1971) and by Hanks (1980) a transition does occur. It is conjectured that the new flow may be a type of complex laminar bifurcation flow described by Joseph (1976), although the present data do not permit a definite conclusion to be reached. This complex laminar flow in turn undergoes a transition to turbulent flow at a second critical Reynolds number, higher than the first, in qualitative accord with Hanks and Bonner's (1971) and Hanks' (1980) predictions, although the latter are not quantitatively correct because they are based on inadequate models of the transitional flow field.

**R. W. HANKS and  
J. M. PETERSON**

Department of Chemical Engineering  
Brigham Young University  
Provo, UT 84602

## SCOPE

The concentric annulus flow geometry is one which has found considerable practical application in the process industries. The concentric annulus also presents a flow system which is still amenable to analysis. In this seemingly simple flow field some rather strange and puzzling phenomena occur. The most interesting of these are associated with the transition from laminar to nonlaminar flow.

Hanks and Bonner (1971) presented extensive experimental data for a number of annuli which showed that the transition from laminar to turbulent flow in concentric annuli occurred over a rather extended range of Reynolds numbers, and that two very distinct critical values of the Reynolds number can be ob-

served. A similar phenomenon had been suspected much earlier by Lea and Tadros (1931) and by Rothfus (1948) and Walker et al. (1957), but the existence of the multiple critical Reynolds numbers had not been clearly demonstrated. The existence of two critical Reynolds numbers had also been predicted theoretically (Hanks and Bonner, 1971; Joseph, 1976; Hanks, 1980).

Rothfus and his coworkers (Rothfus, 1948; Rothfus et al., 1950, 1958; Croop and Rothfus, 1962) observed definite distortions in the shapes of velocity profiles in transitional flows in annuli. In particular they observed that the point of maximum velocity deviated from its theoretical laminar position in a certain definite fashion. This behavior was explained by those authors as being caused by the onset of turbulence in a macroscopic flow region surrounding the core while the flow region lying outside

J. M. Peterson is presently with Signetics Corp., Orem, UT.  
0001-1541-82-6422-0900-\$2.00. © The American Institute of Chemical Engineers, 1982.